Therapeutics and Clinical Risk Management

Dovepress
Taylor & Francis Group

Open Access Full Text Article

ORIGINAL RESEARCH

Modified Alberta Stroke Program Early CT Score (ASPECTS) of Contrast Extravasation on Dual-Energy CT Predicts Haemorrhagic Transformation and Poor Outcome After Endovascular Thrombectomy

Xinyi Chen[1], Jie Xu[2], Sheng Zhang[3], Shunyuan Guo[3], Huiyuan Wang[3], Yafei Shang[3], Panpan Shen[3], Jiawei Ye[3], Yu Geng[3]

[1]Department of Neurology, The Affiliated Hospital of Jiaxing University, Jiaxing, Zhejiang, People's Republic of China; [2]Department of neurology, Huzhou Central Hospital, Huzhou, Zhejiang, People's Republic of China; [3]Department of Neurology, Zhejiang Provincial People's Hospital, Hangzhou, Zhejiang, People's Republic of China

Correspondence: Yu Geng, Department of Neurology, Zhejiang Provincial People's Hospital, 158# Shangtang Road, Hangzhou, Zhejiang, 310014, People's Republic of China, Email gengyu@hmc.edu.cn

Purpose: Haemorrhagic transformation (HT) is an unpredictable complication of acute ischaemic stroke with large vessel occlusion following endovascular thrombectomy (EVT), and imaging parameters that are correlated with haemorrhage are unknown. We developed a modified version of the Alberta Stroke Program Early Computed Tomography Score (ASPECTS) by adding a periventricular region to assess cerebral contrast extravasation (CE) on dual-energy computed tomography (DECT) and assessed its predictive value for HT.

Methods: In total, 101 patients who underwent DECT immediately after EVT were prospectively enrolled. CE was defined as incident hyperdensity on iodine overlay maps. We quantified the CT attenuation in Hounsfield units (HU) and iodine concentration within the CE regions. The modified ASPECTS divided the middle cerebral artery vascular territory into 11 regions and added one region (paraventricular) to the original score. CE was scored as 1 point for each region, and the cumulative score was determined. Follow-up imaging was performed within 7 days postoperatively to confirm the occurrence of HT. A receiver operating characteristic (ROC) curve was constructed to assess the predictive value of various DECT-measured parameters for HT.

Results: Overall, 75/101 (74.3%) patients exhibited CE following EVT, and 47/101 (46.5%) patients exhibited HT. In the ROC curve analysis, the DECT parameter with the maximal area under the curve (AUC) for HT was the modified ASPECTS (AUC=0.87), indicating that patients with a modified ASPECTS >2 were more likely to develop HT (sensitivity: 83.0%, specificity: 83.3%). The maximum iodine concentration (AUC=0.76) and maximum CT attenuation (AUC=0.68) in the hyperdense region were also predictors of postoperative HT.

Conclusion: The modified ASPECTS is a practical and sensitive method for assessing postoperative HT risk in patients following EVT.

Keywords: dual-energy computed tomography, endovascular thrombectomy, ASPECTS, haemorrhagic transformation

Introduction

The efficacy of endovascular thrombectomy (EVT) in patients with acute ischaemic stroke (AIS) with large vessel occlusion (LVO) has been confirmed.[1,2] However, approximately 45% of patients are unable to achieve adequate functional recovery after EVT.[3] A higher incidence of haemorrhagic transformation (HT), especially symptomatic intracranial haemorrhage, after EVT is a key factor.[4,5] Although post-EVT haemorrhage is an important complication, there are currently no accurate methods to predict its occurrence. Contrast extravasation (CE) is a prevalent phenomenon

Received: 7 May 2025
Accepted: 13 November 2025
Published: 1 December 2025

manifested by brain hyperdensity on computed tomography (CT) after EVT, with incidence rates ranging from 15.8% to 85%.[6–8] It is widely believed that haemorrhage results from damage to the basal membrane of the vascular wall, whereas CE occurs when endothelial cells are injured.[9] CE is associated with the opening and disruption of the blood–brain barrier (BBB) and is believed to be related to HT and poor prognosis following reperfusion therapy. Studies based on non-contrast CT (NCCT) have indicated that high CT attenuation clearly visible in the brain contour is associated with an increased likelihood of HT,[10] as haemorrhage and contrast enhancement manifest on NCCT as hyperdensity. NCCT does not presently have a clear CT attenuation threshold that can accurately identify haemorrhage and CE.[11]

Dual-energy CT (DECT) allows differentiation between CE and haemorrhage and provides quantitative information about CE. The maximal iodine concentration[12,13] or the ratio of the maximum iodine concentration to the iodine concentration in the superior sagittal sinus can predict delayed HT following EVT.[14] Nevertheless, owing to differences in CE location and CT attenuation characteristics, the risk of HT may vary.[15,16] Few studies have investigated the relationship between the location and magnitude of iodine leakage and postoperative HT. Iodine overly maps (IOMs) generated by DECT provide additional information on CE; however, the imaging parameters that are correlated with haemorrhage are unknown. This study aimed to develop a practical and sensitive method to semi-quantitatively assess the extent of CE and to compare this method with previously reported indicators. Our results have implications for evaluating the severity of CE and more precisely predicting the risk of postoperative haemorrhagic transformation following EVT.

Materials and Methods

Study Design and Population

From October 2021 to January 2023, we prospectively screened patients with AIS with LVO in the anterior circulation confirmed by CT angiography with onset less than 24 hours from a single centre. Patients enrolled in the study ranged in age from 18 to 90 years and were admitted with a National Institutes of Health Stroke Scale (NIHSS) score of >6. The CT perfusion (CTP) imaging criteria were based on the DEFUSE 3 and DAWN studies.[17] In the absence of contra-indications, patients with a last normal time to onset of <4.5 hours received intravenous recombinant tissue plasminogen activator (rt-PA) (0.9 mg/kg) as a bridge treatment.

Routinely recorded baseline admission data included age, sex, medical history, onset-to-door time, onset-to-reperfusion time, stroke severity (NIHSS score), blood pressure, blood glucose level, and other laboratory indicators.

After providing informed consent, all patients went through a similar EVT procedure, which was performed in accordance with international guidelines. The expanded Treatment in Cerebral Infarction (eTICI) grade was used as an indicator of the degree of reperfusion. The first-pass effect was defined as the attainment of eTICI grade 2c/3 reperfusion after a single pass.

NCCT was performed 24–36 and 72 hours postoperatively to evaluate intracranial haemorrhage, and susceptibility-weighted imaging (SWI) was administered 3–7 days postoperatively. The primary outcome was CT- or SWI-determined HT occurrence within 7 days, with HT classified as HI-1, HI-2, parenchymal haemorrhage (PH)-1, or PH-2 based on the European Cooperative Acute Stroke Study criteria. Patients were followed up for 90 days, and the modified Rankin scale (mRS) score was recorded; a 90-day mRS score ≤2 indicates a good functional prognosis.

Image Protocol

Four-dimensional (4D) time-resolved whole-brain CT and perfusion imaging were performed using an Aquilion 320-slice CT scanner (Toshiba, Tokyo, Japan). All perfusion parameters were analysed using commercial software MIStar (Apollo Medical Imaging Technology, Melbourne, Australia). Foci with relative cerebral blood flow (rCBF) <30% were defined as the ischaemic core. The penumbra volume was calculated by subtracting the ischaemic core volume from the perfusion lesion volume (delay time threshold >3 seconds).

All patients underwent DECT imaging immediately after surgery. A dual-source 256-layer CT scanner (SOMATOM Force, Siemens Healthcare, Forchheim, Germany) was used to acquire DECT images. The following CT parameters were acquired and reconstructed: bulb tube voltage A tube, 90 kV; B tube, 150 kVp; detector collimation, 64×0.6 mm; rotation time, 1.0 second; scan pitch, 0.7; cranial scan direction, caudal-cranial; slice thickness, 0.6 mm; and dose modulation

Care Dose4D was activated with ADMIRE 2 iterative reconstruction algorithms. Using commercial software (syngo CT Dual-Energy Brain Hemorrhage; Siemens), subsequent image post-processing was performed to acquire three images, including a dual-energy hybrid map simulating conventional 120-kV CT, the MIX map (90 kV/150 kV). Virtual noncontrast (VNC) and IOM images were acquired using dual-energy material differentiation, and iodine data subtraction was performed on the initial dataset. All produced datasets were stored in Digital Imaging and Communications in Medicine format.

To assess haemorrhage, a plain monoenergetic CT scan was obtained between 24 and 36 hours and at 72 hours postoperatively, and magnetically sensitive weighted imaging SWI was performed between 3 and 7 days postoperatively.

Image Analysis

Two radiologists with 10 years of experience reviewed and evaluated the images, and quantitative results were determined by aggregating their scores. When the difference between them exceeded 10%, a second measurement was performed.

Patients were assessed for the presence of hyperdense VNC and CE on DECT. Both haemorrhage and CE were hyperdense on the MIX map. Hyperdensity on the VNC images was suggestive of haemorrhage, whereas hyperdensity on the IOM images was suggestive of CE. Subsequently, we classified the CE patterns on the IOM images into cortical, subcortical, cortical, subcortical, and subarachnoid. Additionally, we set the modified Alberta Stroke Program Early Computed Tomography Score (ASPECTS) (Figure 1) and classified the middle cerebral artery vascular territory as periventricular, caudate head, lenticular nucleus, internal capsule, insular cortex, M1, M2, M3, M4, M5, and M6. The presence of CE at each site was scored as 1 point, for a total score of 11 points. The scoring method of the modified ASPECTS differs from the traditional ASPECTS in that a higher score corresponds to a wider distribution of CE. Based on the ASPECTS, we added the periventricular region, which corresponds to the body of caudate nucleus and the periventricular white matter (PVWM). According to previous reports, the low density of the body of caudate nucleus shown on NCCT also be associated with haemorrhage and poor prognosis.[18] In the clinical practice before the commencement of our research, we also observed that this area is one of the common sites for CE. Therefore, we added this scoring area separately to construct a new scale. Figure 2 shows the imaging assessment.

The mean and maximum iodine concentrations were determined by drawing regions of interest (ROIs) on the IOM images simultaneously (Figure 1); the mean iodine concentration was measured by drawing multiple ROIs if there were multiple regions of CE. The mean CT attenuation and maximum CT attenuation of the hyperdense region were determined similarly at the same location on the MIX map. Hyperdense areas with a basal ganglia diameter >1 cm and CT attenuation values ≥90 Hounsfield units were defined as "metallic high-density signs".[19]

Statistical Analysis

The Student's *t*-test (for continuous variables with a normal distribution), Mann–Whitney *U*-test (for continuous variables with an irregular distribution), or χ^2/Fisher's exact test was used to detect differences in baseline characteristics and the performance of CE on DECT images between the HT group and non-HT groups. Additionally, logistic regression analysis was performed to determine whether the DECT imaging parameters were independent risk factors for haemorrhage. A receiver operating characteristic (ROC) curve was used to evaluate the predictive values of the modified ASPECTS, iodine concentration, and CT attenuation in the hyperdense region. The Kruskal–Wallis test was used to compare the maximum iodine concentrations and modified ASPECTS between the different haemorrhage types. IBM SPSS Statistics 23 (IBM Corp., Armonk, NY, USA) was used to perform statistical analyses. Statistical significance was set at $P<0.05$. The ROC analysis was conducted using MedCalc Software (MedCalc Software Ltd., Ostend, Belgium).

Results

Between October 2021 and January 2023, we collected data prospectively from 114 patients with AIS with LVO who were treated with EVT. Six patients did not undergo DECT immediately after EVT due to CT equipment maintenance or respiratory circulation instability. Two patients experienced secondary embolic events during hospitalisation. One patient died of abrupt cardiac arrest, and four patients were lost to follow-up within 3 months of discharge due to accidents or other reasons. Following exclusion, 101 patients (56 males and 45 females) were included in analyses.

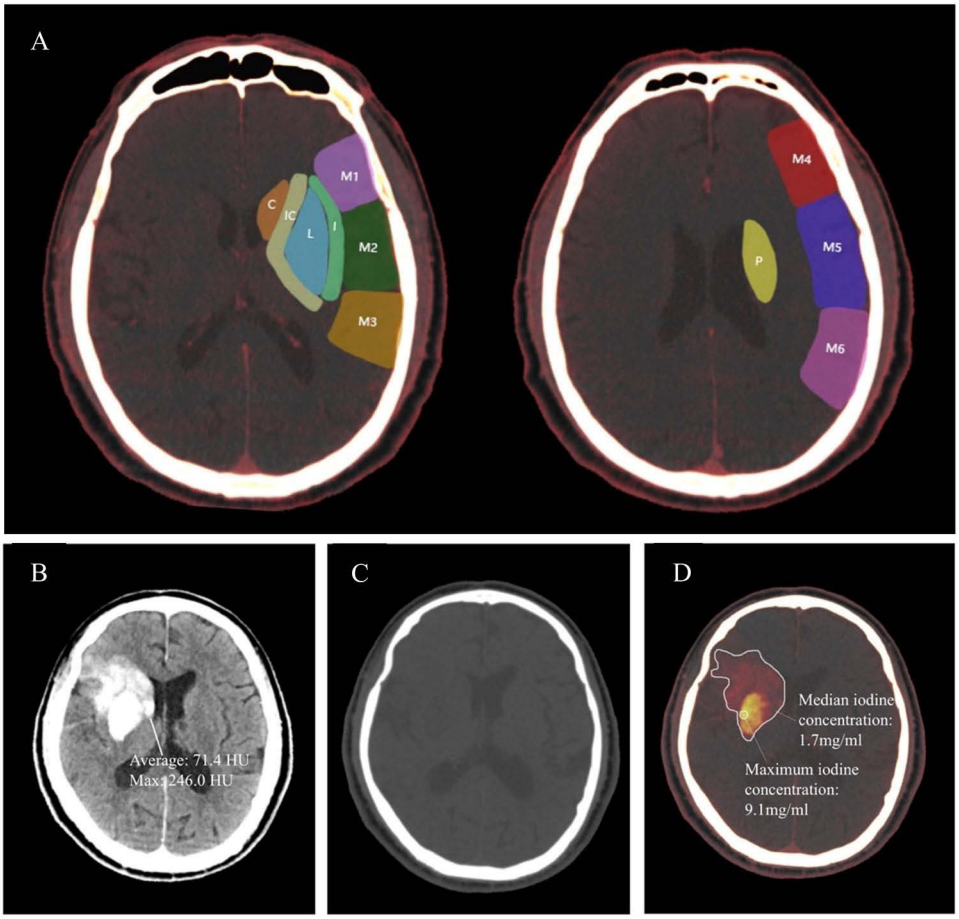

Figure 1 Modified ASPECTS, iodine concentration and CT attenuation in hyperdensities.Modified ASPECTS on the IOM images (**A**). (P) paraventricular; (C) caudate; IC: internal capsule; (L) lenticular nucleus; I: insular cortex. MIX map, with average CT attenuation of 74.1HU, and maximum CT attenuation of 246 HU (**B**). VNC map shows no hyperdensity (**C**). IOM shows the mean iodine concentration is 1.7 mg/mL, and the maximum iodine concentration is 9.1mg/mL. The Modified ASPECTS is 6 (**D**).

The mean age of patients was 68.5±14.4 years, and the median NIHSS score at admission was 14 (interquartile range [IQR], 9–18). The median infarct core volume on preoperative CTP was 20 (IQR, 5.5–43.0) mL. In total, 44/101 (43.6%) patients were treated with rt-PA. Sixty-one (60.4%) patients achieved eTICI grade 2c or 3 recanalisation. The median onset-to-recanalisation time was 440 (range, 307–743) minutes, and the median puncture-to-recanalisation time was 56 (range, 37–77) minutes. Follow-up CT and SWI results within 7 days postoperatively showed that 47 (46.5%) patients had HT, 27 (26.7%) had haemorrhagic infarction (HI), 19 (18.8%) had PH, of which 15 (14.9%) had PH1, 4 (4.0%) had PH2, and 7 (6.9%) had symptomatic intracranial haemorrhage. There was a significant difference in prognosis between patients with and without HT (P<0.001) (Figure 3). Patients with haemorrhage had a higher baseline NIHSS score (P=0.012), larger core infarction volume on CTP (P=0.049), and higher eTICI grade of 2c/3 (P=0.028) than those of patients without haemorrhage (Table 1). Age, sex, medical history, laboratory findings at admission, etiologic typing, and time from onset to recanalisation did not differ significantly between the groups.

In total, 47/101 (46.5%) patients exhibited HT and 75/101 (74.3%) underwent CE after EVT (Table 2). The proportion of CE in patients with HT was significantly higher than that in those without HT (93.6% vs 57.4%, P<0.001). The HT group had a higher maximum iodine concentration (1.8 vs 1.3 mg/mL, P<0.001) and a higher CT attenuation of hyperdense lesions than those in the control (72.3 vs 55.7 HU, P=0.028). However, the groups showed no significant differences in mean iodine concentration or mean hyperdensity attenuation on CT.

A multivariate analysis revealed that cortical with subcortical CE (adjusted odds ratio [aOR]=5.05, 95% confidence interval [CI]=1.64–15.59, P=0.005) was an independent risk factor for the development of HT (Table 2). After further defining the sites of CE, we discovered that patients with CE in the periventricular, caudate head, lenticular nucleus,

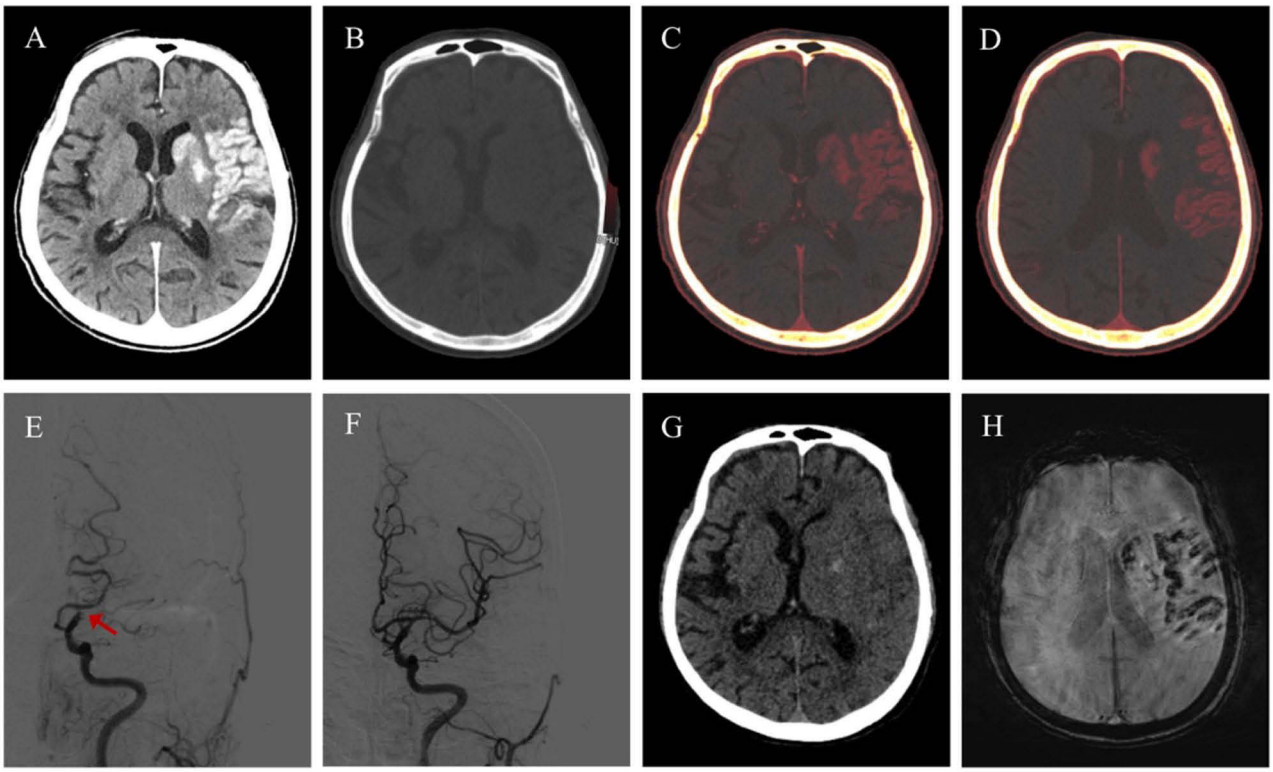

Figure 2 An adult patient with acute occlusion of the C7 segment of the left internal carotidartery ((**E**), the red arrow) underwent mechanical thrombectomy and achieved eTICI grade 2c recanalization (**F**); DECT was performed immediately after recanalization. MIX map revealed multiple hyperdensity regions in the supply area of the left middle cerebral artery (**A**); VNC showed no hyperdense area (**B**); CE was primarily observed in the caudate nucleus, lenticular nucleus, insular cortex, M1, M5 and paraventricular area on IOM. The Modified ASPECTS was 6 (**C** and **D**); the 24-hour postoperative cranial NCCT revealed minor patchy haemorrhage in the basal ganglia (**G**); and the 3-day postoperative SWI revealed patchy haemorrhage foci in the left temporal and parietal lobes, consistent with the area of CE (**H**).

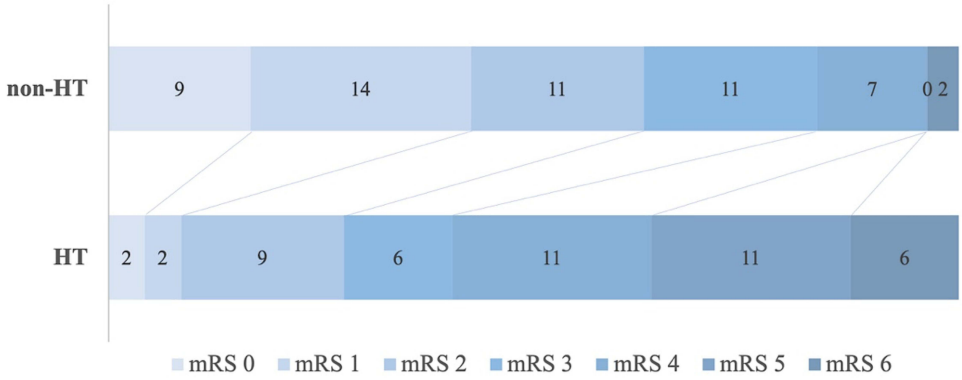

Figure 3 90-day mRS for patients with and without HT.
Abbreviations: HT, haemorrhagic transformation; mRS, modified Rankin scale.

internal capsule, insular cortex, M1, M2, M5, and M6 regions had a markedly increased risk of HT compared with those of patients without the corresponding area of CE. Additionally, a higher modified ASPECTS (aOR=2.20, 95% CI: 1.60–3.03, P<0.001), higher maximum iodine concentration (aOR=2.78, 95% CI: 1.28–6.06, P=0.010), and higher maximum attenuation in hyperdense lesions (aOR=1.03, 95% CI: 1.01–1.06, P=0.06) were significantly associated with an increased risk of HT.

An ROC curve analysis showed that patients with a modified ASPECTS >2 were more likely to develop HT (AUC: 0.87, sensitivity: 82.98%, specificity: 83.33%, positive predictive value: 81.3%, negative predictive value: 84.9%)

https://doi.org/10.2147/TCRM.S522244

Table 1 Characteristics of Patients with and without Hemorrhagic Transformation

Characteristic	Non-HT (n=54)	HT (n=47)	P value
Male, n (%)	31 (57.4)	25 (53.2)	0.671
Age (years), mean±SD	66.9±14.12	70.5±14.66	0.214
Smoking, n (%)	20 (37.0)	16 (34.0)	0.754
Alcohol drinking, n (%)	12 (22.2)	13 (27.7)	0.528
Hypertension, n (%)	38 (70.4)	28 (59.6)	0.255
Diabetes, n (%)	12 (22.2)	11 (23.4)	0.888
Atrial fibrillation, n (%)	20 (37.0)	21 (44.7)	0.435
Hypercholesteremia, n (%)	10 (18.5)	6 (12.8)	0.430
TOAST classification, n (%)			0.116
LAA	25 (46.3)	14 (29.8)	
Cardioembolism	23 (42.6)	27 (57.4)	
Other determined etiology	5 (9.3)	2 (4.3)	
Undetermined etiology	1 (1.9)	4 (8.5)	
SBP (mmHg), mean±SD	154.4±26.89	153.8±33.68	0.913
DBP (mmHg), mean±SD	88.8±18.22	83.9±21.48	0.217
Glucose (mmol/L), mean±SD	8.1±4.37	8.3±2.48	0.769
WBC (10^9/L), mean±SD	9.1±3.33	8.8±3.44	0.585
PLT (10^12/L), mean±SD	192±68.16	190±64.33	0.919
Occlusion site, n (%)			0.284
ICA	17 (31.5)	11 (23.4)	
MCA-M1	27 (50.0)	29 (61.7)	
MCA-M2	8 (14.8)	3 (6.4)	
Tandem occlusion	2 (3.7)	4 (8.5)	
Baseline NIHSS score, median (IQR)	12.5 (9)	15 (8)	0.012
CTP core (mL), median (IQR)	16 (32)	30 (49)	0.049
CTP penumbra (mL), median (IQR)	94 (107)	96 (103)	0.876
ODT (min), median (IQR)	285 (369)	300 (450)	0.300
ORT (min), median (IQR)	449 (349)	425 (540)	0.905
rt-PA, n (%)	20 (37.0)	22 (46.8)	0.320
FPE, n (%)	26 (48.1)	17 (36.2)	0.225
Passes, median (IQR)	2 (2)	2 (2)	0.344
eTICI 2c/3, n (%)	38 (70.4)	23 (48.9)	0.028
24h NIHSS score, median (IQR)	7 (10)	14 (11)	0.001

(*Continued*)

Table 1 (Continued).

Characteristic	Non-HT (n=54)	HT (n=47)	P value
90-day mRS, median (IQR)	2 (2)	4 (3)	<0.001
Good outcome, n (%)	34 (63.0)	13 (27.7)	<0.001

Abbreviations: IQR, interquartile range; SD, standard deviation; LAA, large artery atherosclerosis; SBP, systolic blood pressure; DBP, diastolic blood pressure; WBC, white blood cell count; PLT, platelet; PTA, percutaneous transluminal angioplasty; ICA, internal carotid artery; NIHSS, National Institutes of Health Stroke Scale; mRS, modified Rankin scale score; rt-PA, intravenous recombinant tissue plasminogen activator; ODT, onset to door time; ORT, onset to recanalization time; eTICI, expanded Treatment in Cerebral Infarction Score; FPE, first-pass effect; good outcome: 90-day mRS≤2;

(Table 3 and Figure 4). The original ASPECTS also demonstrated considerable diagnostic performance in predicting HT, with an AUC of 0.78. At the optimal cutoff value of <8, it achieved a sensitivity of 72.92% and a specificity of 81.13%. The optimal threshold for the maximum iodine concentration was 1.8 mg/mL (sensitivity: 54.55%, specificity: 87.10%). In the ROC analysis the modified ASPECTS had a greater AUC; this AUC value was not significantly different from that of the maximum iodine concentration (0.87 vs 0.76, z=1.631, P=0.103) but both were greater than that for the maximum attenuation on the MIX map (0.87 vs 0.68, z=2.49, P=0.0128 and 0.76 vs 0.68, z=2.39, P=0.0171, respectively).

In comparing cerebral haemorrhage subtypes among groups (Figure 5), the median maximum concentration of iodine was 1.85 mg/mL in the HI and PH groups (P=0.919). The median modified ASPECTS scores in the HI and PH groups were 3 and 4, respectively (P=0.236).

Discussion

This study revealed a correlation between postoperative cerebral contrast agent leakage and the development of HT. We observed that the combined cortical and subcortical CE pattern was an independent risk factor for HT. Moreover, the modified ASPECTS, maximum iodine concentration, and maximum attenuation of the hyperdense area were, to varying degrees, predictive of postoperative HT in patients with AIS with LVO. The modified ASPECTS and maximum iodine concentration had high predictive values. However, neither the modified ASPECTS nor the maximal iodine concentration differed significantly between the HI and PH groups.

Notably, 58.7% patients with CE on IOM in the immediate postoperative period developed HT. Only a small percentage of patients (6.9%) had hyperdensities on VNC images, and all had combined CE. Two of the seven patients exhibited hyperdensity on VNC images in the subarachnoid space and showed no postoperative delayed HT. This was most likely due to the rapid metabolism of a small volume of blood with cerebrospinal fluid circulation. Postoperative follow-up CT scans of the remaining five patients revealed haemorrhage outside the hyperdense area on VNC images. Previous studies have implied that VNC hyperintensity in the immediate postoperative period has a limited prognostic value for late HT.[20,21] Hyperintensities on VNC images may be associated with intraoperative manipulation and may not be directly attributed to delayed intracranial haemorrhage, whereas brain CE better indicates that the patient has HT.

To investigate the correlation between the CE area and the risk of HT, we evaluated the contrast distribution pattern and the modified ASPECTS. It is debatable whether cortical or subcortical CE patterns are more likely to demonstrate HT.[22,23] Magnetic resonance perfusion imaging revealed that in patients with subcortical and basal ganglia infarction, intraregional rCBF was lower than that in patients with cortical infarction alone. However, there was no significant difference in the K*trans* value, an index of BBB permeability, between the groups (P>0.05).[24] The risk of HT was substantially increased when the cortex was combined with subcortical CE. In conjunction with the regression analysis of the modified ASPECTS and HT, we hypothesized that a larger area of increased BBB permeability was significantly associated with a higher risk of HT. However, the severity of BBB disruption may not be determined by the volume of CE alone, as a previous study did not find a significant correlation between this parameter and the occurrence of HT (aOR=1.08, P=0.120), and the relationship between the two is disputed.[16,25] Owing to the differences in the degree of hypoxia tolerance at various sites and in the lateral blood supply, it may be more scientific to divide the blood supply according to its functional localisation in the region, rather than to simply measure the CE volume. The ASPECTS covers

https://doi.org/10.2147/TCRM.S522244

Table 2 Univariate and Multivariate Analysis Using Dual-Energy CT Imaging Features as Independent Variables

DECT Imaging Features	Non-HT (n=54)	HT (n=47)	OR (95% CI)	P value	*aOR (95% CI)	P value
CE, n (%)	31 (57.4)	44 (93.6)	10.88 (3.00–39.45)	<0.001	11.82 (3.08–45.36)	<0.001
CE site, n (%)						
Cortical area	2 (3.7)	5 (10.6)	3.10 (0.57–16.77)	0.190	-	-
Subcortical area	11 (20.4)	19 (40.4)	2.65 (1.10–6.41)	0.111	-	-
Cortical + subcortical area	5 (9.3)	18 (38.3)	6.08 (2.04–18.13)	0.001	5.05 (1.64–15.59)	0.005
Subarachnoid space	9 (16.7)	3 (6.4)	0.34 (0.09–1.34)	0.124	-	-
CE locations						
Periventricular	6 (11.1)	29 (61.7)	12.89 (4.59–36.20)	<0.001	12.58 (4.31–36.75)	<0.001
Caudate head	3 (5.6)	12 (25.5)	5.83 (1.53–22.18)	0.010	8.06 (1.99–32.65)	0.003
Lenticular nucleus	13 (24.1)	33 (70.2)	7.43 (3.07–17.98)	<0.001	7.15 (2.81–18.22)	<0.001
Internal capsule	1 (1.9)	13 (27.7)	20.27 (2.53–162.05)	0.005	24.08 (2.89–200.74)	0.003
Insular cortex	4 (7.4)	21 (44.7)	10.10 (3.14–32.52)	<0.001	7.84 (2.36–25.99)	0.001
M1	2 (3.7)	11 (23.3)	7.94 (1.66–38.01)	0.009	7.12 (1.43–35.55)	0.016
M2	4 (7.4)	13 (27.7)	4.78 (1.44–15.91)	0.007	3.68 (1.04–13.01)	0.043
M3	3 (5.6)	3 (6.4)	1.16 (0.22–6.04)	0.861	-	-
M4	3 (5.6)	10 (21.3)	4.60 (1.18–17.86)	0.028	3.48 (0.81–15.01)	0.094
M5	1 (1.9)	9 (19.1)	12.55 (1.53–103.29)	0.019	9.94 (1.14–86.99)	0.038
M6	2 (3.7)	4 (8.5)	2.42 (0.42–13.85)	0.321	-	-
IOM-CE score, median (IQR)	0 (1)	3 (3)	2.28 (1.662–3.115)	<0.001	2.20 (1.60–3.03)	<0.001
Metallic hyperdensity sign, n (%)	0 (0)	11 (23.4)	/	<0.001	-	-
Mean attenuation on MIX map (HU), median (IQR) (n=75)	34.3 (14.1)	40.6 (26.6)	1.02 (0.99–1.04)	0.185	-	-
Maximum attenuation on MIX map (HU), median (IQR) (n=75)	55.7 (20.3)	72.3 (32.7)	1.02 (1.00–1.05)	0.028	1.03 (1.01–1.06)	0.010
Mean iodine concentration (mg/mL), median (IQR) (n=75)	1.3 (0.6)	1.6 (1.2)	1.84 (0.89–3.81)	0.099	-	-
Maximum iodine concentration (mg/mL), median (IQR) (n=75)	1.3 (0.6)	1.8 (1.2)	2.61 (1.19–5.70)	0.016	2.78 (1.28–6.06)	0.010

Note: *Analysis adjusted for: baseline NIHSS, CTP core volume, eTICI 2c/3.

Abbreviations: HT, hemorrhagic transformation; DECT, dual-energy CT; CE, contrast extravasation; VNC, virtual non-contrast; MIX, mix image; HU, Hounsfield Unit; Metallic hyperdensity sign: a nonpetechial intracerebral hyperdense lesion (diameter, ≥1 cm) in the basal ganglia and a maximum CT density of >90 HU; IOM: iodine overlay map.

Table 3 ROC Analysis of Modified ASPECTS, Maximum Iodine Concentration, and Maximum Attenuation of Hyperdensity Areas

Variate	AUC	95% CI	Se	Sp	PPV	NPV	Cut-off Value
Modified ASPECTS	0.867	0.770–0.916	82.98	83.33	81.3	84.9	2
Original ASPECTS	0.782	0.704–0.869	72.92	81.13	77.8	76.8	8
Maximum iodine concentration (mg/mL)	0.757	0.644–0.849	54.55	87.10	85.7	57.4	1.8
Maximum attenuation (HU)	0.677	0.559–0.780	77.27	54.84	70.8	63.0	56.7

Abbreviations: AUC, area under the curve; Se, sensitivity; Sp, specificity; PPV, positive predictive value; NPV, negative predictive value.

most regions supplied by the middle cerebral artery; however, it does not include potential areas where CE may occur after anterior circulation stroke. Anatomically, the paraventricular region primarily comprises the body of the caudate nucleus and the periventricular white matter (PVWM). These territories lack collateral circulation, rendering them vulnerable to ischemic necrosis or hemorrhagic infarction. Notably, our preliminary clinical observations have identified CE in the paraventricular region following EVT in a subset of patients, and this phenomenon is not uncommon. To achieve a more comprehensive assessment of CE distribution, we developed the modified ASPECTS by incorporating the paraventricular region into the original ASPECTS framework. The modified ASPECTS as a new scoring system demonstrated a good ability to predict HT. Its performance might be better than that of original ASPECTS when used to evaluate the distribution area of CE.[15]

Moreover, our study confirmed that the maximum iodine concentration, as opposed to average iodine concentration, was significantly associated with HT.[12] The optimal maximal iodine concentration for predicting HT was 1.8 mg/mL, consistent with previous results.[16] Several DECT parameters could predict HT; however, the modified ASPECTS was more sensitive than the maximum iodine concentration for predicting HT. Iodine concentration is susceptible to variation in various factors; accordingly, small localised hyperpermeabilities do not necessarily show haemorrhage. Alternatively,

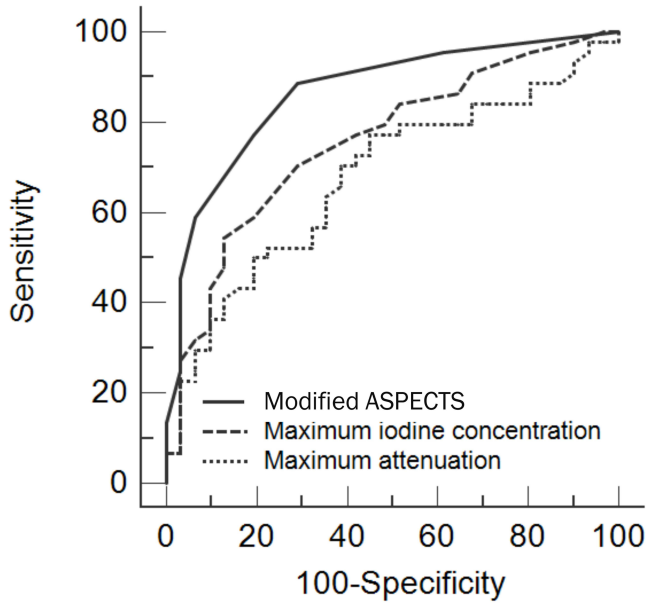

Figure 4 ROC analysis of different DECT parameters to predict HT.
Abbreviations: DECT, dual-energy computed tomography; HT, haemorrhagic transformation.

https://doi.org/10.2147/TCRM.S522244

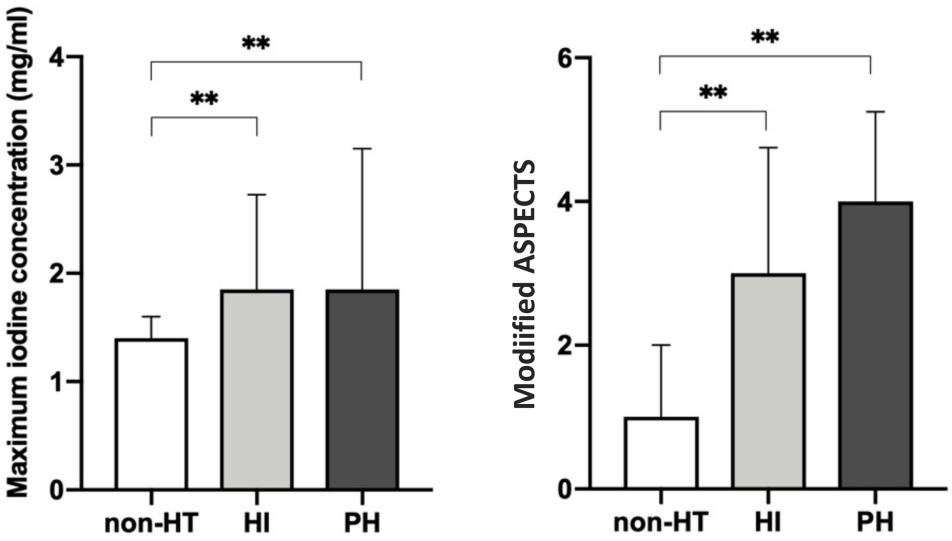

Figure 5 Maximum iodine concentration and Modified ASPECTS in patients with different haemorrhage types. **P<0.001.
Abbreviations: HT, haemorrhagic transformation; HI, haemorrhagic infarction; PH, parenchymal haemorrhage.

if trace haemorrhage is present, it is rapidly metabolised and absorbed and therefore cannot be observed on CT. Thus, the iodine concentration may not comprehensively reflect the severity of ischaemic injury or the modified ASPECTS score.

A haemorrhage subtype analysis indicated that the maximum iodine concentration and modified ASPECTS may not be able to predict and distinguish the severity of HT at present.[13] The median modified ASPECTS was higher in the PH group than in the HI group; however, the difference was not significant. This trend suggests that the occurrence of severe haemorrhagic conversion events may be linked to diffuse contrast agent extravasation as opposed to a significant increase in local permeability. In a previous study, the maximum iodine concentration was not correlated with the haemorrhage volume; however, the iodine extravasation volume was correlated with the final haemorrhage volume.[16]

These results of this study suggest that although some patients present with uncomplicated CE in the immediate postoperative period, they still require urgent medical attention because haemorrhage may be imminent. In patients with high modified ASPECTS and high iodine concentrations, it is necessary to evaluate the need to delay the initiation of antiplatelet or anticoagulant drugs and the ability to intervene with intensive hypotension to reduce the risk of HT. Given the low incidence of high VNC density in the immediate postoperative period and the large number of patients presenting with simple CE, the modified ASPECTS can be performed using NCCT or flat-panel CT in the immediate postoperative period when dual-energy CT assessment is unavailable; however, its accuracy must be validated in future studies.

Our study had a few limitations. First, this was a prospective single-centre nested case-control study with a small sample; therefore, the results require external validation with a larger sample size. Second, the specific focus on patients with symptomatic intracranial haemorrhage prevented us from exploring the association between various CE indicators and severe haemorrhagic events. Third, we assessed intracranial haemorrhage in patients 3–7 days postoperatively using SWI. We detected HI-type haemorrhages in 26.7% of patients; however, microhaemorrhages in the ischaemic area may not necessarily have prognostic value.

Conclusion

Quantitative and semiquantitative evaluations of CE using immediate postoperative DECT can assist clinicians in understanding the risk of postoperative HT. The modified ASPECTS, maximum iodine concentration, and maximum CT attenuation of the hyperintense area were independent predictors of HT, with the modified ASPECTS being the most practical and sensitive evaluation method. Based on our findings, in clinical practice, patients with a modified ASPECTS > 2 or a maximum iodine concentration > 1.8 mg/mL are at a significantly elevated risk of postoperative HT, necessitating intensified clinical

vigilance. This may include more frequent cranial CT monitoring and stricter blood pressure management. Nevertheless, these conclusions await further validation through larger-sample studies. Future investigations remain warranted to elucidate the relationship between CE and the development of HT, cerebral edema, as well as long-term clinical outcomes. Another pertinent research question is whether early intervention based on risk stratification via CE assessment can ultimately improve prognosis through tailored therapeutic adjustments.

Abbreviations

EVT, endovascular thrombectomy; AIS, acute ischaemic stroke; LVO, large vessel occlusion; HT, haemorrhagic transformation; CE, contrast extravasation; CT, computed tomography; BBB, blood–brain barrier; NCCT, non-contrast computed tomography; DECT, dual-energy computed tomography; IOMs, iodine overly maps; NIHSS, National Institutes of Health Stroke Scale; rt-PA, recombinant tissue plasminogen activator; ASPECTS, Alberta Stroke Program Early Computed Tomography Score; SWI, susceptibility-weighted imaging; PH, parenchymal haemorrhage; mRS, modified Rankin Scale; 4D, four-dimensional; rCBF, relative cerebral blood flow; VNC, virtual noncontrast; ROIs, regions of interest; ROC, receiver operating characteristic; IQR, interquartile range; HI, haemorrhagic infarction; vs, versus; aOR, adjusted odds ratio; CI, confidence interval.

Data Sharing Statement

The dataset for this study is available by contacting the corresponding author.

Ethics Statements

Ethical approval for this study was obtained from the Human Ethics Committee of Zhejiang Provincial People's Hospital (No. 2018KY031). All patients provided informed consent before the procedure. The study was conducted according to the Declaration of Helsinki.

Acknowledgments

Thanks are due to Peng Wang and Zongjie Shi for assistance with the interventional operation.

Author Contributions

All authors made a significant contribution to the work reported, whether that is in the conception, study design, execution, acquisition of data, analysis and interpretation, or in all these areas; took part in drafting, revising or critically reviewing the article; gave final approval of the version to be published; have agreed on the journal to which the article has been submitted; and agree to be accountable for all aspects of the work.

Funding

This work was supported by Zhejiang Provincial Science and Technology Department Foundation (No. 2022C35071) and the Supporting Discipline of Neurology in Jiaxing (2023-ZC-006).

Disclosure

The authors declare that they have no known competing financial interests or personal relationships that could have appeared to influence the work reported in this paper.

References

1. Campbell BC, Mitchell PJ, Kleinig TJ, et al. Endovascular therapy for ischemic stroke with perfusion-imaging selection. *New England J Med*. 2015;372(11):1009–1018. doi:10.1056/NEJMoa1414792
2. Goyal M, Demchuk AM, Menon BK, et al. Randomized assessment of rapid endovascular treatment of ischemic stroke. *New England J Med*. 2015;372(11):1019–1030. doi:10.1056/NEJMoa1414905
3. Berkhemer OA, Fransen PS, Beumer D, et al. A randomized trial of intraarterial treatment for acute ischemic stroke. *New Engl J Med*. 2015;372(1):11–20. doi:10.1056/NEJMoa1411587

4. Hao Y, Zhang Z, Zhang H, et al. Risk of intracranial hemorrhage after endovascular treatment for acute ischemic stroke: systematic review and meta-analysis. *Int Neurol*. 2017;6(1–2):57–64. doi:10.1159/000454721
5. Goyal M, Menon BK, van Zwam WH, et al. Endovascular thrombectomy after large-vessel ischaemic stroke: a meta-analysis of individual patient data from five randomised trials. *Lancet*. 2016;387(10029):1723–1731. doi:10.1016/s0140-6736(16)00163-x
6. Lummel N, Schulte-Altedorneburg G, Bernau C, et al. Hyperattenuated intracerebral lesions after mechanical recanalization in acute stroke. *AJNR Am J Neuroradiol*. 2014;35(2):345–351. doi:10.3174/ajnr.A3656
7. Ma C, Hui Q, Gao X, et al. The feasibility of dual-energy CT to predict the probability of symptomatic intracerebral haemorrhage after successful mechanical thrombectomy. *Clin. Radiol*. 2021;76(4):316.e9–316.e18. doi:10.1016/j.crad.2020.12.013
8. Tijssen MP, Hofman PA, Stadler AA, et al. The role of dual energy CT in differentiating between brain haemorrhage and contrast medium after mechanical revascularisation in acute ischaemic stroke. *Eur Radiol*. 2014;24(4):834–840. doi:10.1007/s00330-013-3073-x
9. Renu A, Amaro S, Laredo C, et al. Relevance of blood-brain barrier disruption after endovascular treatment of ischemic stroke: dual-energy computed tomographic study. *Stroke*. 2015;46(3):673–679. doi:10.1161/STROKEAHA.114.008147
10. Jang YM, Lee DH, Kim HS, et al. The fate of high-density lesions on the non-contrast CT obtained immediately after intra-arterial thrombolysis in ischemic stroke patients. *Korean J Radiol*. 2006;7(4):221–228. doi:10.3348/kjr.2006.7.4.221
11. Dekeyzer S, Nikoubashman O, Lutin B, et al. Distinction between contrast staining and hemorrhage after endovascular stroke treatment: one CT is not enough. *J Neurointerv Surg*. 2017;9(4):394–398. doi:10.1136/neurintsurg-2016-012290
12. Bonatti M, Lombardo F, Zamboni GA, et al. Iodine extravasation quantification on dual-energy ct of the brain performed after mechanical thrombectomy for acute ischemic stroke can predict hemorrhagic complications. *AJNR Am J Neuroradiol*. 2018;39(3):441–447. doi:10.3174/ajnr.A5513
13. Ma C, Xu D, Hui Q, Gao X, Peng M. Quantitative intracerebral iodine extravasation in risk stratification for intracranial hemorrhage in patients with acute ischemic stroke. *AJNR Am J Neuroradiol*. 2022;43(11):1589–1596. doi:10.3174/ajnr.A7671
14. Byrne D, Walsh JP, Schmiedeskamp H, et al. Prediction of hemorrhage after successful recanalization in patients with acute ischemic stroke: improved risk stratification using dual-energy ct parenchymal iodine concentration ratio relative to the superior sagittal sinus. *AJNR Am J Neuroradiol*. 2020;41(1):64–70. doi:10.3174/ajnr.A6345
15. Chang GC, Ma DC, Li W, et al. Contrast enhancement by location and volume is associated with long-term outcome after thrombectomy in acute ischemic stroke. *Sci Rep*. 2022;12(1):16998. doi:10.1038/s41598-022-21276-3
16. Baik M, Cha J, Ahn SS, et al. Dual-energy computed tomography quantification of extravasated iodine and hemorrhagic transformation after thrombectomy. *J Stroke*. 2022;24(1):152–155. doi:10.5853/jos.2021.03391
17. Albers GW, Marks MP, Kemp S, et al. Thrombectomy for stroke at 6 to 16 hours with selection by perfusion imaging. *New Engl J Med*. 2018;378(8):708–718. doi:10.1056/NEJMoa1713973
18. Khalaf HS, Ahmed SY, Kurman AJ. Caudate body (CB) sign: new early CT sign of hyperacute anterior cerebral circulation infarction. *Emerg radiol*. 2011;18:533–538. doi:10.1007/s10140-011-0979-y
19. Xu C, Zhou Y, Zhang R, et al. Metallic hyperdensity sign on noncontrast ct immediately after mechanical thrombectomy predicts parenchymal hemorrhage in patients with acute large-artery occlusion. *AJNR Am J Neuroradiol*. 2019;40(4):661–667. doi:10.3174/ajnr.A6008
20. Gao X, Hui Q-T, Li Y-D, et al. Semiquantitative assessment of iodine extravasation in acute ischemic stroke after mechanical thrombectomy. *Chinese Med J*. 2021;134(4):469–471. doi:10.1097/cm9.0000000000001236
21. Cai J, Zhou Y, Zhao Y, et al. Comparison of various reconstructions derived from dual-energy CT immediately after endovascular treatment of acute ischemic stroke in predicting hemorrhage. *Eur Radiol*. 2021;31(7):4419–4427. doi:10.1007/s00330-020-07574-2
22. Kim JM, Park KY, Lee W, et al. The cortical contrast accumulation from brain computed tomography after endovascular treatment predicts symptomatic hemorrhage. *Eur JNeurol*. 2015;22(11):1453–1458. doi:10.1111/ene.12764
23. Yang Y, MTJCn T. Angiogenesis and blood-brain barrier permeability in vascular remodeling after stroke. *Curr Neuropharmacol*. 2020;18(12):1250–1265. doi:10.2174/1570159X18666200720173316
24. Wu L, Liu Y, Zhu L, et al. MRI arterial spin labeling in evaluating hemorrhagic transformation following endovascular recanalization of subacute ischemic stroke Frontiers in Neuroscience. 2023 17 ;1105816 doi:10.3389/fnins.2023.1105816.
25. Li L, Huo M, Zuo T, Wang Y, Chen Y, Bao Y. Prediction of intracerebral hemorrhage after endovascular treatment of acute ischemic stroke: combining quantitative parameters on dual-energy ct with clinical related factors. *J Stroke Cerebrovascular Dis*. 2021;30(10):106001. doi:10.1016/j.jstrokecerebrovasdis.2021.106001